Intermittency of droplet growth in phase separation of off-critical polymer mixtures

Hiroyuki Takeno and Takeji Hashimoto

Citation: The Journal of Chemical Physics **108**, 1225 (1998); doi: 10.1063/1.475484
View online: http://dx.doi.org/10.1063/1.475484
View Table of Contents: http://scitation.aip.org/content/aip/journal/jcp/108/3?ver=pdfcov
Published by the AIP Publishing

Intermittency of droplet growth in phase separation of off-critical polymer mixtures

Hiroyuki Takeno and Takeji Hashimoto[a)]
Department of Polymer Chemistry, Graduate School of Engineering, Kyoto University, Kyoto 606-01, Japan

(Received 9 July 1997; accepted 10 October 1997)

Kinetics of the phase separation in binary off-critical mixtures of polybutadiene (PB) and polyisoprene (PI) was investigated as a function of quench depth and composition by using time-resolved light scattering. The kinetics for the off-critical mixtures is much slower than that for the critical mixture. The scattering maximum for the off-critical mixtures is very broad relative to that for the critical mixture. For the off-critical mixtures, the domain growth follows the same power law ($q_m \sim t^{-\alpha}$, $I_m \sim t^{\beta}$: $\alpha = 0.25-0.33$, $\beta = 0.75-1$) in the long time limit covered in our experiments, independent of quench depth and composition. However, the domain growth became very slow before the long time limit under a certain condition (intermittency of the domain growth). In the regime where the intermittency was observed, the scaling exponents α and β depend on quench depth. The shallower the quench, the smaller the values of α and β and the longer the intermittent regime. These behaviors are largely different from those for the critical mixture for which the scaling exponents show almost the same value in the late stage for different quenches and the Langer–Bar-on–Miller or Chou–Goldburg scaling postulate is fulfilled. Scaled structure factor in the late stage of phase separation process was found to depend on quench depth, becoming broader as quench is shallower. © *1998 American Institute of Physics.* [S0021-9606(98)52203-9]

I. INTRODUCTION

Phase separation kinetics in polymer mixtures has been extensively studied by numerous researchers in the past few decades.[1–3] Time evolution of phase separating domains is traditionally characterized by the scaling law,

$$q_m \sim t^{-\alpha}, \tag{1}$$

$$I_m \sim t^{\beta}, \tag{2}$$

where q_m and I_m are the peak wave number and the scattering maximum, respectively. α and β are the scaling exponents characterizing the time-evolution. In the intermediate stage of spinodal decomposition (SD), as the characteristic wavelength and amplitude of the concentration fluctuations increase with time, the relation between α and β is given by

$$\beta > 3\alpha. \tag{3}$$

On the other hand, in the late stage of SD, the amplitude of the concentration fluctuations reaches the equilibrium value determined by the coexisting curve. Therefore, the relation between α and β is given by

$$\beta = 3\alpha. \tag{4}$$

The scaling postulate in the phase separation process was proposed by Langer–Bar-on–Miller (LBM) and Chou–Goldburg (CG).[4,5] Namely, the plot between the wave number $Q_m[=q_m/q_m(0)]$ and the time $\tau(=t/t_c)$ reduced by a characteristic wave number $q_m(0)$ and a characteristic time t_c, respectively, at various quench depth superimposes onto a single mater curve.

In addition, the scaled structure factor $F(x,t)$ is defined by[6]

$$F(x,t) = q_m(t)^3 I(x,t) = \langle \eta^2(t) \rangle S(x,t), \tag{5}$$

and

$$x = q/q_m(t). \tag{6}$$

$I(x,t)$ and $\langle \eta^2(t) \rangle$ are the scattering function and the space-averaged square of refractive index fluctuations at a given time t, respectively. $S(x,t)$ is a scaling function at time t which characterizes a shape of growing structure. q is wave number which is defined by $q = (4\pi/\lambda)\sin(\theta/2)$, where θ and λ are the scattering angle and the wavelength in the medium, respectively. In the late stage, if the kinetics of phase separation obeys the dynamic scaling hypothesis, $\langle \eta^2(t) \rangle$ becomes constant with t, and $S(x,t)$ becomes independent of t, and hence $F(x,t)$ becomes an universal function.

According to Flory–Huggins model[7,8] based on mean-field theory, the free energy $f(\phi_A)$ per lattice site of polymer mixtures on mixing is given by

$$\frac{f(\phi_A)}{k_B T} = \frac{\phi_A \ln \phi_A}{N_A} + \frac{(1-\phi_A)\ln(1-\phi_A)}{N_B} + \chi \phi_A (1-\phi_A), \tag{7}$$

where N_i and ϕ_i are degree of polymerization and volume fraction of ith component ($i = A$ or B), respectively, ($\phi_A + \phi_B = 1$). χ is the Flory–Huggins interaction parameter. k_B and T are used in the usual meaning. χ parameter is often described by the following experimental form:

$$\chi = s + \frac{h}{T}. \tag{8}$$

[a)]Author to whom correspondence should be addressed.

Spinodal points which show stability limit can be calculated from Eq. (7), i.e., $[\partial^2 f(\phi_A)/\partial\phi_A^2]=0$ at spinodal point. In the region inside spinodal curve, phase separation takes place via spinodal decomposition (SD).[9] Here, even infinitesimal concentration fluctuations lead to decrease of free energy of the system and therefore grows with time. In the region between binodal and spinodal curve, phase separation occurs according to nucleation and growth (NG).[10] Here, the disordered state is metastable, i.e., thermally activated small concentration fluctuations decay because they increase the free energy of the mixture, while thermal concentration fluctuations greater than a critical one cause decrease of free energy, and therefore they grow with time.

Phase separation dynamics is strongly affected by the mechanism of the phase separation. Therefore, a change in phase separation mechanisms, if it occurs, causes the change in the phase separation dynamics. However, crossover phenomena from one mechanism to another have not been sufficiently understood at present. In the previous paper, we reported on the crossover in the dynamics from that relevant to a growth of percolated morphology to that relevant to a growth of droplet morphology, i.e., crossovered dynamics associated with percolation-to-cluster transition (PCT).[11] Before the PCT takes place, the phase separation grows according to the power law with an exponent of $\alpha=0.9$ which is close to that predicted for the growth of percolated morphology.[12] After the PCT occurred, the phase separation kinetics became very slow.[11,13,14] Afterwards, in the much longer time, the kinetics proceeds with the growth law of droplets ($\alpha=1/4-1/3$).[6,15,16]

In this paper, we report on a new crossover phenomena where the phase separation kinetics becomes very slow in off-critical quenches (''intermittency'' of the domain growth). At first sight, this crossover phenomenon appears to be the same behavior as that caused by PCT. However, it is shown that the intermittency of the domain growth is not caused by PCT, if we elaborately analyze the results.

II. EXPERIMENT

A. Sample preparation and characterization

PB and PI were polymerized by living anionic polymerization. The PB has a weight-averaged molecular weight (M_w) of 5.8×10^4 and the polydispersity index for the molecular weight distribution M_w/M_n of 1.2, respectively, where M_n is a number-averaged molecular weight. The PI has a M_w of 10.1×10^4 and M_w/M_n of 1.3, respectively. The microstructures of the PB and PI were reported in the previous paper.[11] Blend specimens were dissolved in toluene in $\sim2\%-3\%$ by total polymer weight fraction. After the solution was filtered by a milipore film with a pore size of 0.45 μm, solvent was slowly evaporated. In addition, the films prepared were dried under vacuum for 2 days in order to perfectly remove the solvent. The films were put on a clear glass plate and then degassed under vacuum for ~12 h in order to remove bubbles. The films were sandwiched between two clear glass plates for light scattering measurements and the thickness was 0.5 mm.

B. Cloud points

Cloud points were determined by using light scattering. As the kinetics of phase separation in the PB/PI mixtures is very slow, especially in the off-critical mixtures, we determined the cloud points by comparing a scattering profile in a homogeneous state with that after annealing for more than one week at a given temperature. Namely, if the scattering intensity after annealing at a given temperature increased more than that before annealing, we assessed that the mixture was in two-phase region at this temperature. Otherwise, it was assessed to be in single-phase region. Cloud points were obtained by carrying out such measurements as described above for various compositions and temperatures.

C. Time-resolved light scattering

By using time-resolved light scattering method, we studied time-evolution of phase separation after the mixture was transferred from a homogenous state into a two-phase state by a temperature jump. Measurements were performed for PB/PI mixtures having compositions of 74.7/25.3 and 80/20 wt. %/wt. %. Hereafter, we designate the composition of A/B wt. %/wt. % as A/B for simplicity. The time-evolution of the domain growth for the 50/50, 65/35, and 70/30 mixture was reported in the previous paper.[11]

The scattering profile, $I_s(q)$, in the single-phase state before quench into the two-phase region was measured for each quench experiment. The measured scattering profile $I_s(q)$ was subtracted from the scattering profiles after quench, $I(q,t)$, in order to remove the scattering due to artifact, e.g., impurities in sample and so on. All the scattering data shown in the following sections, except for scattering profiles in Fig. 2, are corrected for the scattering profile in the single-phase state $I_s(q)$.

III. RESULTS AND DISCUSSION

A. Calculation of binodal and spinodal curves

Cloud points for the PB/PI mixtures are shown in Fig. 1 (open circles). As shown in Fig. 1, the mixtures have a lower critical solution temperature (LCST) type phase diagram, i.e., while at temperatures below the cloud point the mixture is in the single-phase state, at temperatures above the cloud point the mixture is in the two-phase state. In addition, we show the binodal curve which was obtained by a best fit of Flory–Huggins theory to the measured cloud points. s and h of Eq. (8) are parameters for the fit. The values of s and h obtained are 0.00628 and -1.38, respectively. These values are close to those obtained by small-angle neutron scattering (SANS) measurement for a blend of the same PI as that used in this study and deuterated PB (DPB) which has almost the same microstructure and molecular weight as those of the PB used in this study. The values of s and h obtained by the SANS measurement for the DPB/PI 50/50 mixture are 0.00454 and -1.02, respectively.[17] Moreover, mean-field spinodal curve in the context of Flory–Huggins theory was calculated by using the values of s and h (Fig. 1). However, we should notice that in fact, it is very difficult to directly

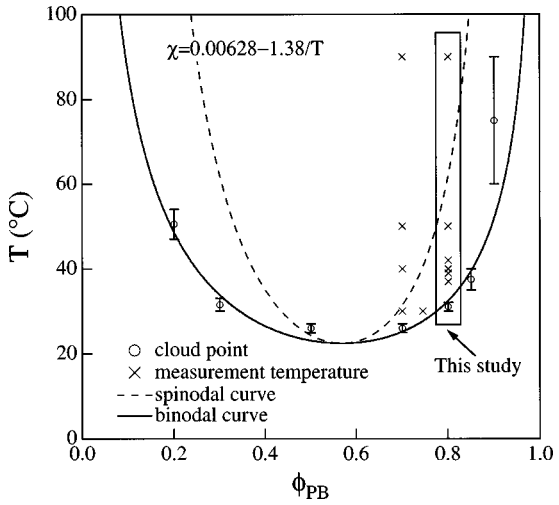

FIG. 1. Cloud points, spinodal, and binodal curves. The latter two curves were calculated in the context of Flory–Huggins theory based on the assumption that the χ parameter is independent of composition. The phase separation experiments were carried out at the points marked by ×.

determine spinodal points from the phase separation process, i.e., distinction of SD from NG near the spinodal curve is difficult as Binder pointed out.[18]

B. Time-evolution of scattering profiles

Figure 2 shows time-evolution of scattering profiles after quench into two-phase region for the 80/20 mixture at (a) $T=39\,^{\circ}\mathrm{C}$ and (b) $T=90\,^{\circ}\mathrm{C}$. Cloud point for the 80/20 mixture is $T=31\pm1\,^{\circ}\mathrm{C}$. It is shown in Fig. 2 that, at both temperatures, a scattering maximum appears, and it increases

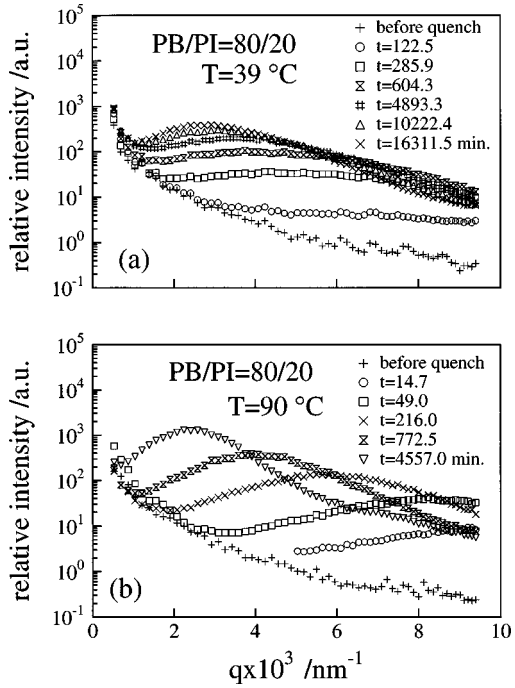

FIG. 2. Time evolution of scattering profiles for 80/20 wt. %/wt. % (a) at $T=39\,^{\circ}\mathrm{C}$ and (b) 90 °C.

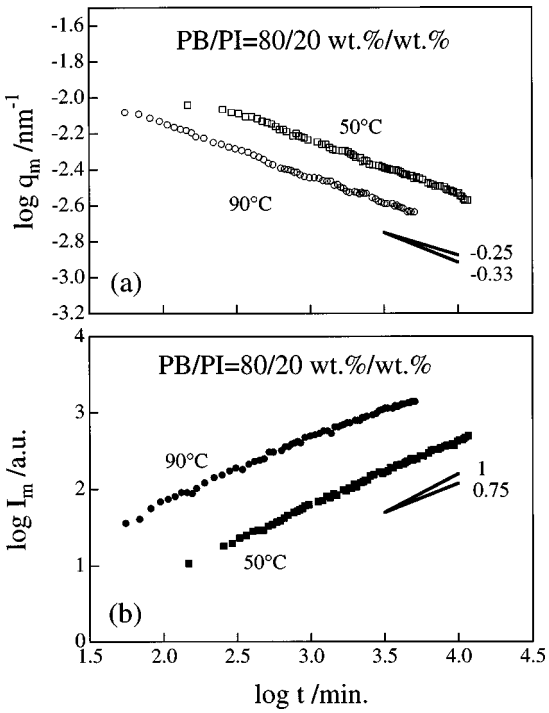

FIG. 3. Time evolution of (a) q_m and (b) I_m for 80/20 wt. %/wt. % at deep quenches.

and shifts toward low q with time. At $T=39\,^{\circ}\mathrm{C}$, the peak shift toward low q with time becomes slow after $t=604.3$ min. However, at $T=90\,^{\circ}\mathrm{C}$, such slowing down of the peak shift is not observed. The time change in q_m at these temperatures will be reported in details in the following section. Furthermore, the scattering peak at $T=39\,^{\circ}\mathrm{C}$ is broader than that at $T=90\,^{\circ}\mathrm{C}$.

C. Time-evolution of q_m and I_m

Figure 3 shows double logarithmic plot of (a) q_m vs time t and (b) I_m vs t for the 80/20 mixture at deep quenches ($T=50$ and 90 °C). The exponents α and β in Eqs. (1) and (2) at both temperatures show 0.25–0.33 and 0.75–1, respectively, in the late time. The same trend was observed for the 70/30 mixture.[11] The exponents α and β for the 70/30 mixture showed the same values, or 0.25–0.33 and 0.75–1, respectively, in both shallow and deep quenches ($T=30-90\,^{\circ}\mathrm{C}$) in the long time limit covered in our experiment.[11] Their values are close to those expected from the growth of droplets by evaporation-condensation mechanism (Lifsitz–Slyozov–Wagner law) or diffusion-coalescence of droplets with hydrodynamic interactions ($\alpha=1/3$).[6,15,16] This 1/3 power law has also been experimentally found by Okada *et al.*[19] and L. Sung *et al.*[20] for off-critical mixtures of polystyrene/poly(2-chlorostyrene) and deuterated polystyrene/polybutadiene, respectively. Therefore, the phase separated structures at these temperatures for the 80/20 mixture are expected to form droplets morphology.

On the other hand, the time changes in q_m and I_m at shallow quenches ($T=42$, 40, 39, and 37 °C) for the 80/20 mixture are quite different from those at deep quenches

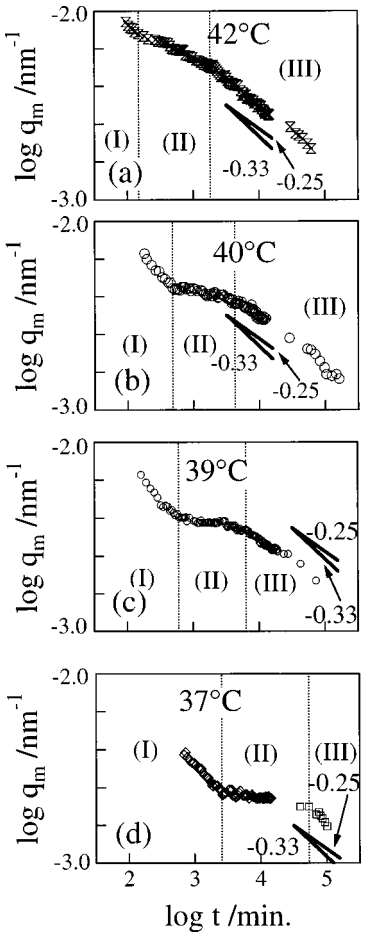

FIG. 4. Time evolution of q_m for 80/20 wt. %/wt. % at shallow quenches.

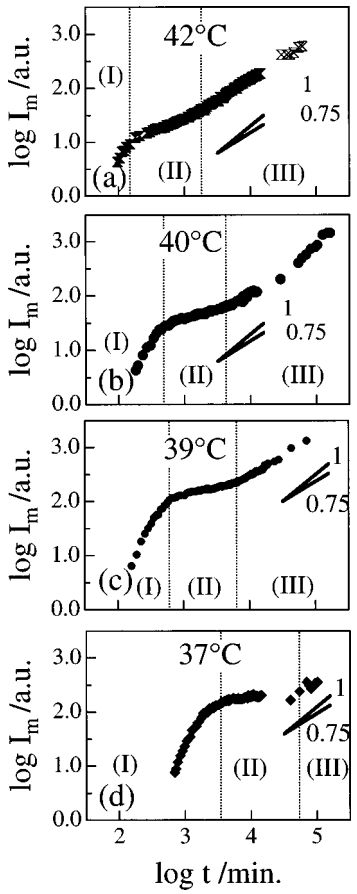

FIG. 5. Time evolution of I_m for 80/20 wt. %/wt. % at shallow quenches.

($T=90$ and 50 °C). As shown in Fig. 4, the time change in q_m at (a) $T=42$, (b) 40, (c) 39, and (d) 37 °C can be divided into three regimes [regime (I)–(III)]. Similarly, Fig. 5 shows that the time change in I_m at (a) $T=42$, (b) 40, (c) 39, and (d) 37 °C can also be divided into three regimes. In regime (I), α and β have 0.32–0.37 and 1.70–2.50, respectively, as shown in Fig. 6(a). The relation between α and β fulfills inequality (3) [Fig. 7(a)]. Therefore, in regime (I), concentration fluctuations do not reach an equilibrium value yet and hence increases with time. In another words, the growing droplets have not reached the equilibrium compositions yet. In regime (II), the growth of the phase separated structure becomes very slow (intermittency of the droplet growth). Namely, α and β are very small and they are 0.04–0.18 and 0.18–0.51, respectively, as shown in Fig. 6(b). Here, it is important to note that the values of α and β in regime (II) depend on quench depth. The shallower the quench (the lower the temperature), the smaller the values of α and β, i.e., the slower the time-evolution of phase separation. Moreover, the shallower the quench, the longer the regime (II), as may be recognized in Fig. 4.

The quench-depth dependence of α and β implies that the validity of LBM and CG scaling postulate[4,5] does not hold for the 80/20 mixture. This behavior is largely different from that for the critical mixture of the same PB/PI (Ref. 21) and other critical mixtures[22–24] in which LBM and CG scaling postulate holds.

Here, it might be possible to consider that the intermittency of the droplet growth in regime (II) is related to the ''spontaneous pinning of the domain growth'' caused by PCT.[11,13] However, we should notice that the behavior is different from that due to PCT in some respects. As the quench-depth becomes shallower, the $q_{m,\mathrm{II}}$, at which regime (II) begins, becomes smaller. Moreover, the time t_{II}, at which regime (II) begins, is later in shallower quench (Figs. 4 and 5). These results are quite opposite to those caused by PCT. In the case of PCT, the shallower the quench-depth, the earlier PCT occurs, and the larger the $q_{m,p}$ at which PCT takes place.[11,13] In addition, PCT took place for the 65/35 mixture of the PB/PI in our light scattering experiment.[11,25] It is predicted from these results that the intermittent growth in regime (II) is not caused by PCT. In regime (III) which is the long time limit covered in these measurements, the phase separation dynamics shows the same behaviors as those at deep quenches for the 80/20 mixture and for the 70/30 mixture. Namely, the scaling exponents α and β show 0.25–0.33 and 0.75–1, respectively, in the long time as shown in Fig. 6(c). It is shown in Fig. 7(c) that β/α is almost equal to 3 at all temperatures in regime (III). Hence the growing droplets have reached equilibrium compositions in regime (III).

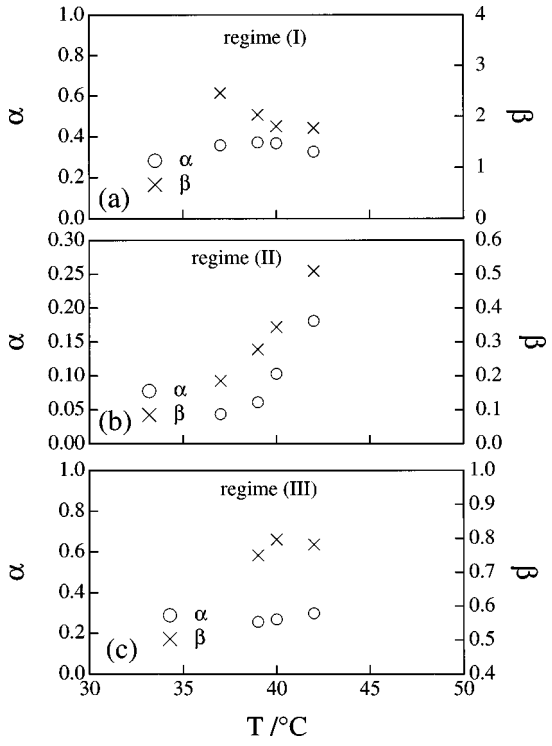

FIG. 6. Scaling exponents α and β as a function of temperature in each regime.

D. Scaled structure factor at deep and shallow quenches

We present time change in the scaled structure factor $F(x,t)$ for the 80/20 mixture at $T=50\,^{\circ}\mathrm{C}$ (a deep quench) in Fig. 8. In Fig. 8(a) obtained at $t\leqslant 393.2$ min, $F(x,t)$ increases with time at whole x region, indicating that $\langle \eta^2(t)\rangle$ grows with time. Figure 8(b) shows that $F(x,t)$ in the late time $t\geqslant 905.5$ min becomes a universal function. Apart from the form of $F(x,t)$, this universal behavior in the late time is similar to that for the critical mixture.[21]

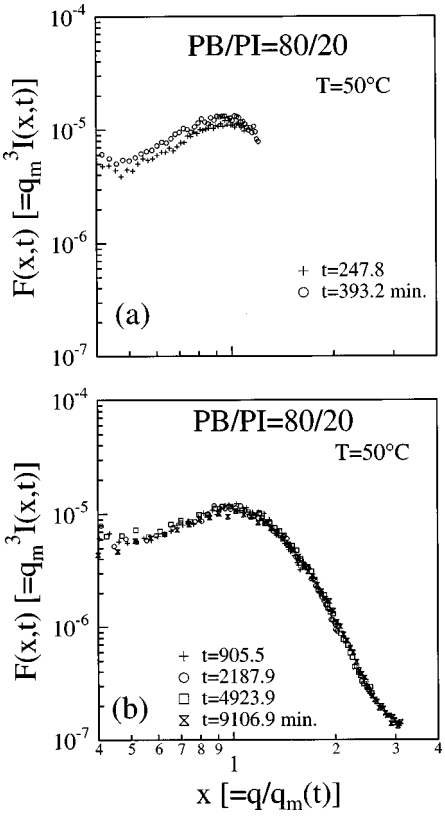

FIG. 8. Time change in scaled structure factor $F(x,t)$ at $T=50\,^{\circ}\mathrm{C}$.

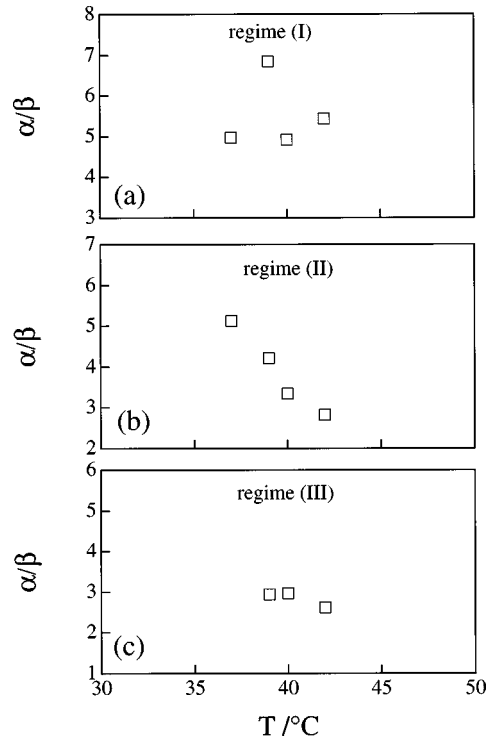

FIG. 7. α/β as a function of temperature in each regime.

Figures 9(a)–9(c) show the double logarithmic plot of $F(x,t)$ vs x in regime (I)–(III), respectively, at $T=42\,^{\circ}\mathrm{C}$ (a shallow quench) for the 80/20 mixture. Similar plots at $T=40\,^{\circ}\mathrm{C}$ (a shallow quench) are shown in Figs. 10(a)–10(c). In Figs. 9(a) and 10(a), $F(x,t)$ increases with time at whole x region in regime (I), suggesting that $\langle \eta^2(t)\rangle$ becomes larger with time as expected from Eq. (5). In regime (II), the $F(x,t)$ is independent of t at $x\geqslant 1$, while the $F(x,t)$ is nonuniversal with t at $x<1$ [Figs. 9(b) and 10(b)]. It is predicted from this result that $\langle \eta^2(t)\rangle$ reaches the value near to an equilibrium one in regime (II). However, the scattering function cannot be scaled with the peak wave number q_m. We predict that, in regime (II), the droplets which almost reached the equilibrium compositions, change the spatial distribution with time. In regime (III), $F(x,t)$ is universal with t at whole x region [Figs. 9(c) and 10(c)], which implies that, in regime (III), $\langle \eta^2(t)\rangle$ reaches an equilibrium value and the phase separated structures can be scaled with a single characteristic parameter $\Lambda=2\pi/q_m$. Here, it is important to notice that the system which forms droplets has at least two characteristic length, i.e., interdroplet distance and droplet radius. The peak at $x=1$ is considered to be due to the interference of scattered waves from droplets. This consider-

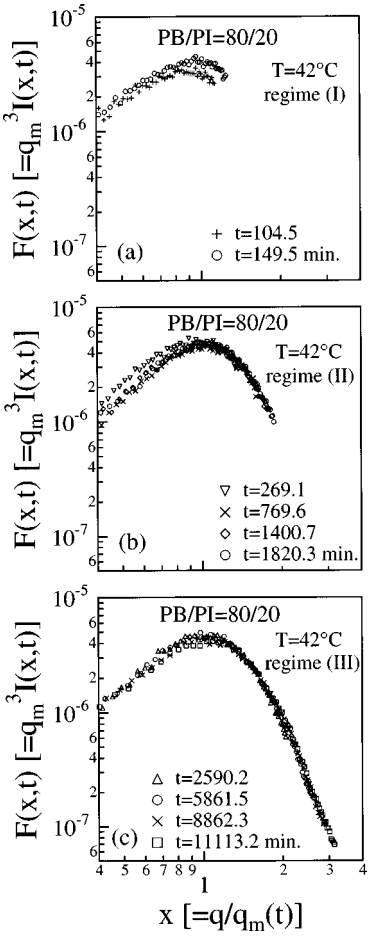

FIG. 9. Time change in scaled structure factor $F(x,t)$ in each regime at $T=42\,^{\circ}\mathrm{C}$.

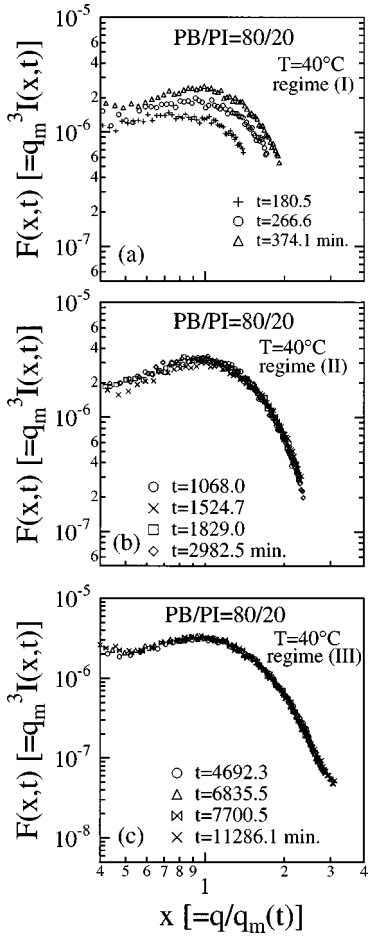

FIG. 10. Time change in scaled structure factor $F(x,t)$ in each regime at $T=40\,^{\circ}\mathrm{C}$.

ation is based upon the fact that the peak caused by form factor of single droplets was observed in higher-q at $T=37\,^{\circ}\mathrm{C}$ and $T=39\,^{\circ}\mathrm{C}$ in the late time. This result about the scattering of single droplets will be described in the following section.

From the results of the time change in q_m, I_m, and $F(x,t)$, we interpret the behaviors in each regime as follows. In regime (I), as $\langle \eta^2(t)\rangle$ does not reach an equilibrium value, droplets are expected to grow mainly by diffusion of PI molecules from the matrix into droplet phase (PI-rich phase). In regime (III), $\langle \eta^2(t)\rangle$ reaches an equilibrium value and droplets grow according to the diffusion-coalescence of droplets or Lifsitz–Slyozov–Wagner law. We will show our speculation of regime (II) in Sec. III G.

E. Scattering maximum arising from form factor of single droplets

Figure 11(a) shows the scattering profiles after $t=1749.1$ min for the 80/20 mixture at $T=37\,^{\circ}\mathrm{C}$. In addition to a large peak at $q\approx 0.002\ \mathrm{nm}^{-1}$ due to the interdroplet interference effect, a small peak appears at $q\approx 0.009\ \mathrm{nm}^{-1}$. We conjecture that the small peak is caused by the scattering maximum from single droplets. The value of the peak wave number at $t=1749.1$ min corresponds to the droplet radius 0.64 μm under the assumption that the single droplet is spherical. Figure 11(b) presents magnification around the small peak. As shown in Fig. 11(b), the peak intensity increases with time and the peak wave number slightly shifts toward small q, i.e., droplet size gets larger with time. Time-evolution of radii of the droplets, R is presented as follows:

$$R\sim t^{0.025}. \tag{9}$$

F. Quench-depth dependence of scaled structure factor

Figure 12 shows double logarithmic plot of scaled structure factor $F(x,t)$ in the late time, which is normalized by $F(x=1,t)$ for the 80/20 mixture at various quenches, vs x. For the comparison, the $F(x,t)/F(1,t)$ for the 50/50 mixture at $T=33\,^{\circ}\mathrm{C}$ is also shown in Fig. 12. All the $F(x,t)/F(1,t)$ data except for that at $T=37\,^{\circ}\mathrm{C}$ in Fig. 12 are observed in regime (III), where $F(x,t)$ is independent of time. Therefore, in the time region, the size and spatial distributions of the droplets are expected not to change with time for a given ΔT. However, they may depend on ΔT. The form of $F(x,t)/F(1,t)$ for the 80/20 mixture is broader than that for the 50/50 mixture. The $F(x,t)/F(1,t)$ for the 50/50 mixture shows the $x^{-7.5}$ dependence at $1<x<2$ and x^4 dependence

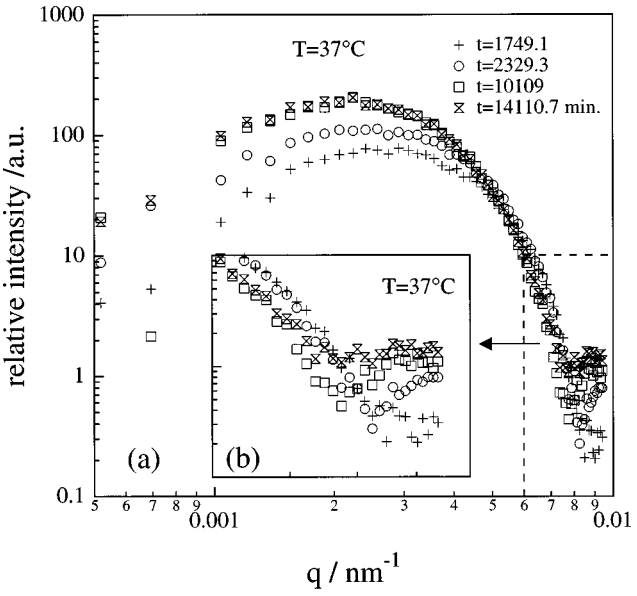

FIG. 11. (a) Scattering function showing the scattering maximum from the form factor of single droplets and (b) the magnification around the scattering maximum.

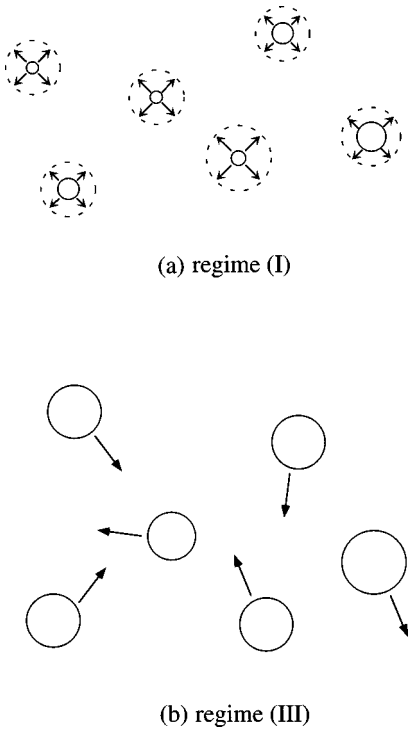

FIG. 13. A possible model for the intermittent growth. (a) Nucleation of droplets and growth of droplets in regime (I) before the two phases attain the equilibrium compositions; in this process centers of droplets may be essentially fixed, and the PI droplets grow via diffusion of PI molecules in the matrix to the droplets. (b) Diffusion-coalescence of droplets in regime (III) after both the droplets and matrix attain the equilibrium compositions. The intermittency of the growth occurs as a result of a switching of the growth mechanism from that in regime (I) to that in regime (III).

at $x<1$, which implies that the phase separated structure is bicontinuous.[11] On the other hand, the $F(x,t)/F(1,t)$ for the 80/20 mixture depends on quench-depth. The form of the $F(x,t)/F(1,t)$ is broader, as quench is shallower. The result is different from that for the 50/50 mixture which is near the critical mixture. In the 50/50 mixture, the scaled structure factor normalized by $\langle \eta^2(t)\rangle$ was universal with quench depth.[21]

We believe that our observation on the broadening of the scaled structure factor with decreasing the quench depth results from a decreasing volume fraction of droplets. It is well expected from the phase diagram shown in Fig. 1 that the volume fraction of the droplets phase decreases with decreasing the quench depth. The trend we observed was able to be qualitatively confirmed even by the simplest model of Debye hard spheres. In the model the scattering function is given by

$$I(q)\sim\langle\eta^2\rangle V_s\Phi V_{\mathrm{drop}}P^2(u)[1-8\Phi P(2u)]. \tag{10}$$

V_s is the total volume of the system, Φ is the volume fraction of spheres, V_{drop} is the volume of a sphere, and $P^2(u)$ is the form factor of single spheres ($u=qR$; R is radius of sphere). Based on Eq. (10), we clearly found the observed trend that the scaled structure factor calculated from Eq. (10) broadens with decreasing Φ, although the results are not included here.

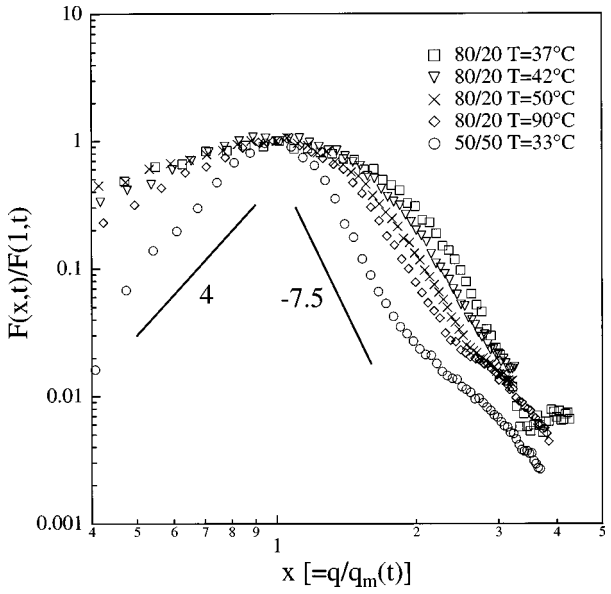

FIG. 12. Scaled structure factor $F(x,t)$ normalized by $F(x=1,t)$ for the 80/20 mixture at various quench depths.

G. A possible model for intermittent growth

At this stage we present our speculation about a possible model of the intermittent growth of droplets in Fig. 13. The droplets (PI-rich phase) may be developed via nucleation and growth. They have a composition very close to an equilibrium composition but the composition of the matrix phase (PB-rich phase) is still far from an equilibrium composition. They grow as a consequence of diffusion of PI molecules in the matrix phase into them but their centers of mass may be essentially fixed (see the growth of the droplets from the particles shown by solid lines to those shown by broken lines in part a). The growth of the PI droplets due to the absorption of PI in the matrix may be much faster than the rate of

TABLE I. Characteristic parameters estimated from Eq. (12) and the light scattering analysis.

T(°C)	$D_{\rm drop}$ (10^{-18} m^2 s^{-1})	$t_{\rm int}$ (10^5 s)	$D_{\rm drop}t_{\rm int}$ (10^{-14} m^2)	$\Lambda_{m,\rm II}^2$(m^2) (10^{-14} m^2)
42	8.66	1.00	0.866	0.69
40	8.47	2.28	1.93	2.03
39	8.37	3.49	2.92	2.42
37	8.21	31.2	25.6	7.30

translational diffusion of droplets themselves. This process causes the PB-rich matrix phase to attain equilibrium composition. After the system (closely) attains the equilibrium composition, the droplets may grow via the mechanism of diffusion-coalescence of droplets as schematically shown in part b. A switching of the growth mechanism (from that shown in part a to that in part b) may possibly explain the intermittency. If this is the case, the intermittent time, $t_{\rm int}$, may correspond to an average time required for the diffusion of particles over an averaged nearest-neighbor distance $\Lambda_{m,\rm II}(=2\pi/q_{m,\rm II})$ at the end of regime (I) [at the beginning of regime (II)],

$$t_{\rm int}\approx\Lambda_{m,\rm II}^2 D_{\rm drop}^{-1}=(2\pi/q_{m,\rm II})^2 D_{\rm drop}^{-1}, \tag{11}$$

where $q_{m,\rm II}$ and $D_{\rm drop}$ are a characteristic wave number and a translational diffusivity of the droplets formed in the system at the end of regime (I). The model explains the experimental observations that $t_{\rm int}$ decreases as T increases, i.e., as T increases (quench becomes deeper), $q_{m,\rm II}$ and $D_{\rm drop}$ increases and therefore $t_{\rm int}$ decreases. Furthermore, we estimated $D_{\rm drop}$ at each temperature where regime (II) was observed, from the following equation:

$$D_{\rm drop}=k_B T/(6\pi\eta R_{\rm drop,II}), \tag{12}$$

where k_B and η are the Boltzmann constant and the viscosity of the matrix, respectively. $R_{\rm drop,II}$ is the radius of the droplet at the end of regime (I). As for the value of η, we used the magnitude of complex dynamic viscosity of the neat PB in the low angular frequency region which were obtained from the dynamic mechanical measurements. On the other hand, as we could not estimate $R_{\rm drop,II}$ at each temperature, we assumed that $R_{\rm drop,II}$ at each temperature equals that (0.6 μm) at $T=37$ °C. Here, we estimated the value of $R_{\rm drop,II}$ at $T=37$ °C from the peak position of the single droplet as shown in Sec. III E. Thus, estimated $D_{\rm drop}$, $t_{\rm int}$, $D_{\rm drop}t_{\rm int}$, and $\Lambda_{m,\rm II}^2$ at each temperature are summarized in Table I. In Table I, $D_{\rm drop}\,t_{\rm int}$ is shown to be approximately close to $\Lambda_{m,\rm II}^2$ at each temperature, supporting qualitatively our model.

One may wonder if the droplets growth according to the scheme shown in Fig. 13(a) can account for the decrease of q_m in regime (I). The trend of the decreasing q_m value with the growth of droplet radii can be predicted even by the simplest model of Debye's hard sphere as discussed in Sec. III F. As radii increase, the form factor $P^2(u)$ shifts toward a small q and the interference part $[1-8\Phi P(2u)]$ shifts slightly toward a large q side [see Eq. (10)]. The two factors give a shift of q_m toward a small q. In fact, we can calculate

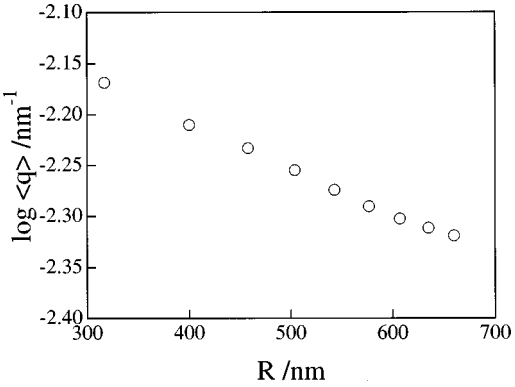

FIG. 14. Plot of $\langle q\rangle$ calculated on the basis of hard sphere model for some sets of (R,Φ)[=(317, 0.01), (400, 0.02), (458, 0.03), (504, 0.04), (543, 0.05), (577, 0.06), (607, 0.07), (635, 0.08), and (660, 0.09)] against R.

the first moment of the intensity distribution of q-fourier mode, $\langle q\rangle$, as functions of R and Φ from the model of Debye's hard sphere [Eq. (10)], where $\langle q\rangle$ is defined by

$$\langle q\rangle=\frac{\int_0^\infty qI(q)q^2dq}{\int_0^\infty I(q)q^2dq}. \tag{13}$$

The $\langle q\rangle$ calculated for some sets of (R,Φ) is plotted against R in Fig. 14. [Note that R and Φ are not independent in our scheme shown in Fig. 13(a), i.e., $(R_2^3/R_1^3)=(\Phi_2/\Phi_1)$ for arbitrary sets of (R_1,Φ_1) and (R_2,Φ_2) holds.] The value $\langle q\rangle$ is shown to decrease with increase of R, by about the same order of magnitude on the results shown in regime (I) in Fig. 4. Thus, the decrease of q_m in the regime (I) can be explained even in the simple model of Debye's hard sphere apart from the value of the scaling exponent α.

Furthermore, a very simple model in Fig. 13(a) assumes no coalescence of droplets or vaporization–condensation mechanism. However, in real systems the mechanisms discussed above may take place to some degree even in regime (I), in addition to the primary mechanism of diffusion of PI molecules in the matrix phase into the droplets.

The above factor(s) are expected to shift q_m toward small q in regime (I). As the future work for the check of our speculation we need real-space observation, which has now been planned in our laboratory.

IV. CONCLUSIONS

The phase separation dynamics for off-critical mixtures of PB and PI was investigated by means of time resolved light scattering. For the 80/20 mixture, the phase separation at shallow quenches seemingly occurs via nucleation and growth (NG) process, and after all, the process can be classified into four regimes, i.e., (i) early stage (nucleation stage), (ii) intermediate stage, (iii) intermittent stage, (iv) late stage. In this study, the early stage where nucleation takes place, is not observed. For the study of the nucleation stage, we should investigate the scattering in higher q, e.g., by using small-angle neutron scattering or x-ray scattering. In intermediate stage after nucleation stage which corresponds to regime (I), droplets rich in PI grow through the diffusion

of PI molecules in the matrix to the droplets, i.e., mean square of refractive index fluctuations increase with time. In late stage which corresponds to regime (III), the exponents, α and β show 0.25–0.33 and 0.75–1, respectively. That is, the droplets and matrix attain their equilibrium composition, and the droplets grow according to diffusion-coalescence with hydrodynamic interactions or Lifsitz–Slyosov–Wagner law. In the intermittent stage, the phase separation dynamics becomes very slow at shallow quenches. The intermittent growth may be caused by the switching of the growth mechanism from that in the intermediate stage to that in the late stage.

ACKNOWLEDGMENT

The authors thank Mr. K. Matsuzaka, Hashimoto Polymer Phasing Project, ERATO, JST, Japan for helping with rheological experiments of PB.

[1] K. Binder, Adv. Polym. Sci. **112**, 181 (1994).
[2] T. Hashimoto, Phase Transit. **12**, 47 (1988).
[3] F. S. Bates and P. Wiltzius, J. Chem. Phys. **91**, 3258 (1989).
[4] J. S. Langer, M. Bar-on, and H. D. Miller, Phys. Rev. A **11**, 1417 (1975).
[5] Y. Chou and W. I. Goldburg, Phys. Rev. A **20**, 2105 (1979).
[6] K. Binder and D. Stauffer, Phys. Rev. Lett. **33**, 1006 (1974).
[7] P. J. Flory, J. Chem. Phys. **9**, 660 (1941).
[8] M. L. Huggins, J. Chem. Phys. **9**, 440 (1941).
[9] J. W. Cahn and J. E. Hilliard, J. Chem. Phys. **28**, 258 (1958).
[10] J. W. Cahn and J. E. Hilliard, J. Chem. Phys. **31**, 688 (1959).
[11] H. Takeno and T. Hashimoto, J. Chem. Phys. **107**, 1634 (1997).
[12] E. D. Siggia, Phys. Rev. A **20**, 595 (1979).
[13] T. Hashimoto, T. Takenaka, and T. Izumitani, J. Chem. Phys. **97**, 679 (1992).
[14] J. Läuger, R. Lay, and W. Gronski, J. Chem. Phys. **101**, 7181 (1994).
[15] I. M. Lifshitz and V. V. Slyozov, J. Phys. Chem. Solids **19**, 35 (1961).
[16] C. Z. Wagner, Electrochemie **65**, 581 (1961).
[17] H. Takeno, H. Jinnai, H. Hasegawa, and T. Hashimoto (in preparation). The miscibility of the PB/PI is different from that of the DPB/PI, due to the isotope effect. In fact, critical temperature of the PB/PI is lower than that of the DPB/PI by $\sim 60\,^{\circ}\mathrm{C}$. Therefore, it is natural that χ parameter of the PB/PI is slightly different from that of the DPB/PI.
[18] K. Binder, Phys. Rev. A **29**, 341 (1984).
[19] M. Okada, J. Sun, J. Tao, T. Chiba, and T. Nose, Macromolecules **28**, 7514 (1995).
[20] L. Sung and C. C. Han, J. Polym. Sci. Part B: Polym. Phys. **33**, 2405 (1995).
[21] M. Takenaka and T. Hashimoto, J. Chem. Phys. **96**, 6177 (1992).
[22] H. L. Snyder and P. Meakin, J. Chem. Phys. **79**, 5588 (1983).
[23] T. Hashimoto, M. Itakura, and N. Shimidzu, J. Chem. Phys. **85**, 6773 (1986).
[24] H. Yang, M. Shibayama, R. S. Stein, N. Shimidzu, and T. Hashimoto, Macromolecules **19**, 1667 (1986).
[25] H. Takeno, E. Nakamura, and T. Hashimoto, J. Chem. Phys. (to be submitted).